The Spheroid Light Microscopy Image Atlas for morphometrical analysis of three-dimensional cell cultures

scientific data

OPEN

DATA DESCRIPTOR

The Spheroid Light Microscopy Image Atlas for morphometrical analysis of three-dimensional cell cultures

Eva Blondeel[1], Arne Peirsman[1,2,3] ✉, Stephanie Vermeulen[1], Filippo Piccinini[4,5], Felix De Vuyst[1], Diogo Estêvão[6,7], Sayida Al-Jamei[8], Martina Bedeschi[4], Gastone Castellani[5], Tânia Cruz[6], Sándor Dedeyne[1], Maria José Oliveira[6], Satoru Kawakita[3], Huu Tuan Nguyen[3], Leoni A. Kunz-Schughart[8,9], Soojung Lee[10], Noemi Marino[4], Patrick Steigemann[11], Shuichi Takayama[10], Anna Tesei[4], Nina Zablowsky[11], Phillip Blondeel[2] & Olivier De Wever[1] ✉

The application of three-dimensional (3D) cell cultures such as spheroids and organoids is growing in popularity both in academia and industry. However, morphology of the 3D architecture remains remarkably understudied. Here, we introduce an open-access Spheroid Light Microscopy Image Atlas (SLiMIA) that can serve as a training set for morphology studies of 3D cell cultures. We provide images with a variety of metadata: 9 microscopes, 47 cell lines, 8 culture media, 4 spheroid formation methods and multiple cell seeding densities; totalling approximately 8,000 images of spheroids. This comprehensive dataset can guide spheroid researchers and promote economizing of resources by advancing 3D cell culture optimization, standardization and implementation by the community at large. Considering the exponentially growing interest in spheroid morphometrical analyses and the emerging technological possibilities to do so, this atlas can be applied to train and develop image segmentation models to deepen our understanding of 3D spheroid morphometry in biomedical research.

Background & Summary

When adherent cells are suspended into single cells and exposed to an environment to which they cannot attach, they tend to self-assemble into three-dimensional (3D) multicellular aggregates or spheroids. Compared to two-dimensional (2D) cell cultures, cells in spheroids experience *in vivo*-like intercellular interactions such as cell crowding, and gradients of oxygen, carbon dioxide, nutrients and waste products[1]. All these phenomena result in a phenotype that better resembles *in vivo* cells[2,3]. Similar to 2D cell cultures, 3D multicellular aggregates show a cell line specific morphometry. Single cell suspensions from different cell lines, seeded at equal numbers in ultra-low attachment (ULA) plates give rise to spheroids that vary in size, circularity, compactness and other

[1]Laboratory of Experimental Cancer Research (LECR), Ghent University, Ghent, Belgium. [2]Plastic, Reconstructive and Aesthetic Surgery University Hospital Ghent, Ghent, Belgium. [3]Terasaki Institute for Biomedical Innovation, Los Angeles, California, 90064, USA. [4]IRCCS Istituto Romagnolo per lo Studio dei Tumori (IRST) "Dino Amadori", Meldola, Italy. [5]Department of Experimental, Diagnostic and Specialty Medicine (DIMES), University of Bologna, Bologna, Italy. [6]Tumour and Microenvironment Interactions group, i3S – Institute for Research & Innovation in Health, Porto UnSiversity, Porto, Portugal. [7]ICBAS – Institute of Biomedical Sciences Abel Salazar, Porto University, Porto, Portugal. [8]OncoRay – National Center for Radiation Research in Oncology, Faculty of Medicine and University Hospital Carl Gustav Carus, TU Dresden and Helmholtz- Zentrum Dresden–Rossendorf, Dresden, Germany. [9]National Center for Tumor Diseases (NCT), Partner Site Dresden, Dresden, Germany. [10]Wallace H. Coulter Department of Biomedical Engineering and Parker H. Petit Institute of Bioengineering and Bioscience, Georgia Institute of Technology, Atlanta, GA, USA. [11]Lead Discovery, Nuvisan ICB GmbH, Muellerstr. 178, 13342, Berlin, Germany. ✉e-mail: arne.peirsman@ugent.be; olivier.dewever@ugent.be

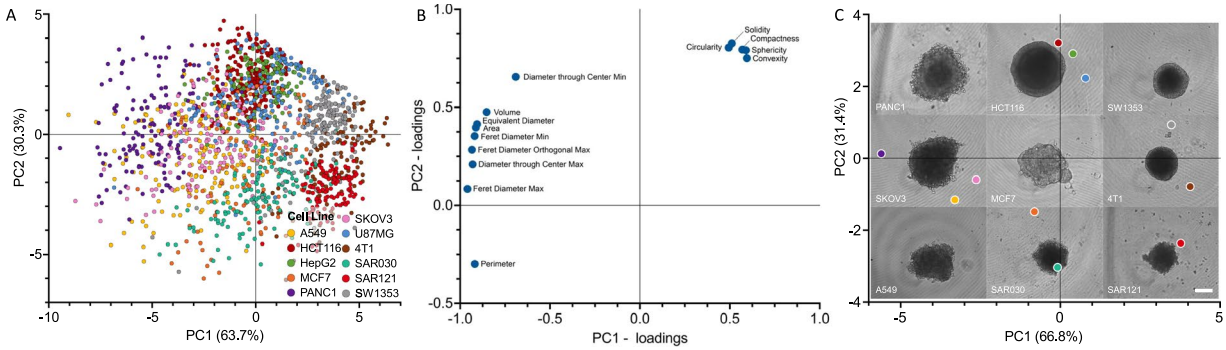

Fig. 1 Diversity of spheroid morphology based on cell type. (**A**) Scatter plot of the first two principal components shows the diversity in spheroid morphology between cell types. Each dot represents a spheroid. (**B**) Loading plot of PCA shows underlying relationship between AnaSP spheroid morphology metrics and how the metrics steer the direction of the principal components. (**C**) PCA scatter plot of the cell types morphology metric averages, supported by illustrative spheroid images. Visualized cell types (9 out of 11) are indicated on the spheroid image. Scale bar = 200 µm, representative for all images. Note: 1 A describes all data, 1 C averages; as a consequence, scales and PC values differ slightly.

morphometrical parameters. To demonstrate this, we performed a principal component analysis (PCA) of frequently used particle morphometrics measured on light microscopy images from spheroids (>1600) of 11 cell cultures used in the MISpheroID study. The analysis shows distinct clustering from large and compact HCT116 spheroids to small and loose SAR121 spheroids (Fig. 1).

Light microscopy is the most accessible way to visualize and assess spheroid morphometry. More than half (54.7%) of all reported (3,058) experiments in the MISpheroID knowledgebase use light microscopy images to analyze spheroid characteristics[4]. Note that light microscopy images are 2D projected images of the 3D object which may fail to capture the full complexity of spheroids. The widespread use of light microscopy imaging stimulated us to create SLiMIA: the Spheroid Light Microscopy Image Atlas. SLiMIA provides the largest open-access 3D cell culture image database with 7,990 images of spheroids from 47 cancer and non-cancer cell lines including methodological metadata such as cell source, cell seeding densities, culture media and spheroid formation methods (Fig. 2, Table 1), allowing researchers to search the dataset as needed. The dataset can be accessed, viewed and downloaded through Figshare[5]. Furthermore, multiple initiatives show increasing attention in morphological cell studies[6–8]. Accordingly, SLiMIA can be applied to compare spheroid diversity and to develop morphometric analysis software with potential applications on other 3D cultures such as organoids and patient-derived tissue fragments.

High-quality image datasets with a wide diversity in spheroid morphotypes are required to develop and optimize performant 3D cell aggregate segmentation platforms and convolutional networks. Reusing existing datasets could form an opportunity to economize both time and resources. Moreover, according to recent developments and guideline proposals, the reuse of light microscopy data will receive a strong boost from the bioimaging community[9,10], consistent with the FAIR (Findable, Accessible, Interoperable, Reusable) principles[11].

Lastly, further research is needed to translate spheroid morphotypes (e.g. circularity/sphericity, compactness, and size) into methodological metadata such as cell source and cell seeding density. In previous work we have shown that spheroid size impacts biological metadata (e.g. cell death, ATP production, cytokine release)[4] and studies are needed to investigate which spheroid morphotype parameters influence spheroid biology. Future atlases may focus on images from drug-treated spheroids that are disintegrated or are obscured by a rim of cell debris[12]. Z-projected images of spheroids allow investigation of the 3D geometry of spheroids and may even further differentiate in distinguishing cell source and spheroid biology[7,13]. In conclusion, SLiMIA is a dataset comprising approximately 8,000 images and has an enormous potential to assist in the development, training and validation of spheroid segmentation models and to connect spheroid morphometry with methodological metadata.

Methods

Cell origin and culture. For uniformity and clarity, cell line names are written in their simplest and most economic notation, with respect to the synonyms registered in the Cellosaurus database[14].

The following cell lines: 4T1 (CRL-2539), A549 (CCL-185), BEAS2B (CRL-3588), BT20 (HTB-19), DLD1 (CCL-221), FaDu (HTB-43), H1299 (CRL-5803), HCT116 (CCL-247), HCT15 (CCL-225), HEK293 (CRL-1573), HEPG2 (HB-8065), Hs578T (HTB-126), MCF7 (HTB-22), MCF10A (CRL-10317), MDAMB231 (HTB-26), MDAMB361 (HTB-27), MRC5 (CCL-171), NCIH226 (CRL-5826), NCIH460 (HTB-177), PANC1 (CRL-1469), SKOV3 (HTB-77), SW837 (CCL-235), SW1353 (HTB-94), T47D (HTB-133), U87MG (HTB-14) and VcaP (CRL-2876) were purchased from the American Type Culture Collection (ATCC, catalog number between brackets). ASC (adipose-derived stem cells) (SCC038) was purchased from Sigma Aldrich (Germany), CAL33 (ACC447) was purchased from DSMZ (Germany), CT5.3 hTERT are hTERT-immortalized cancer-associated fibroblasts of which primary culture was originally isolated from colorectal carcinoma[15–17]. D2A1LUCmCherry was a gift from C. Isacke (London, England)[18], HCA2hTERT are hTERT-immortalized fibroblast of which primary culture was originally isolated from human foreskin (a gift from C. Jones; Cardiff,

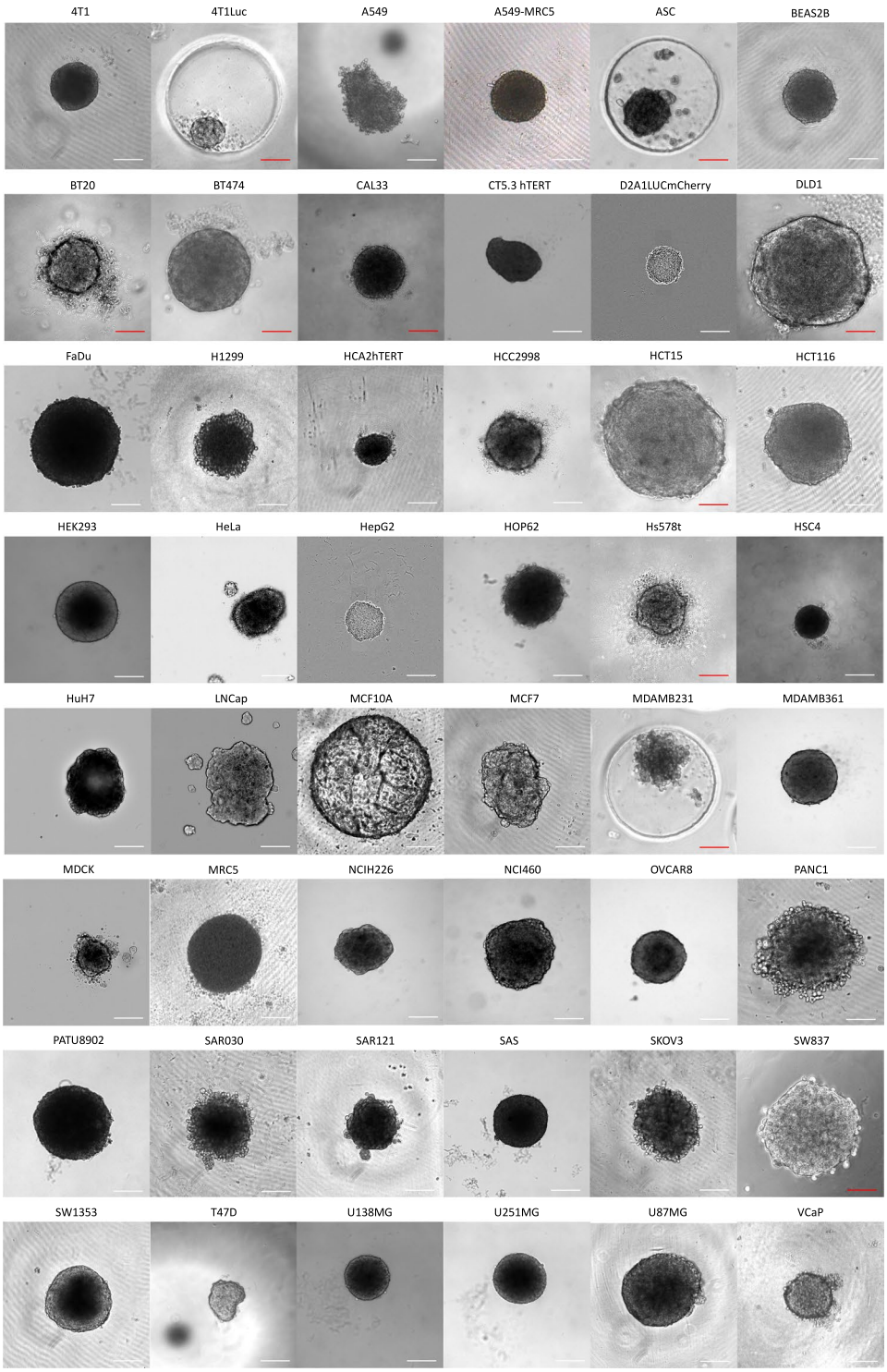

Fig. 2 Cell lines represented in SLiMIA. A snapshot of spheroid images of 47 cancer and non-cancer cell lines available in SLiMIA. It is important to note that cell seeding densities, spheroid formation methods, culture media and timepoint of imaging are variable between presented spheroid images. White scalebar = 200 µm, red scalebar = 100 µm.

UK)[19], HCC2998, HOP62 and OVCAR8 were obtained from National Cancer Institute (NCI, Frederick, USA). HeLa (940003-P-T) was purchased from Tebu-Bio (Paris, France), HSC4 (JCRB0624) and SAS (JCRB0260) was purchased from Japanese Collection of Research Bioresources (JCRB, Japan). HuH7 (300156), MDCK (602280), U138MG (300363) and U251MG (300385) were purchased from Cell Line Service (CLS) GmbH (Germany). SAR030 and SAR121 are early passage soft tissue sarcoma cell cultures as previously described[4,20].

For clarity, 2D cell culture conditions prior to spheroid formation are summarized in Table 2.

Microscope	Cell Line	Culture Medium	Formation Method	Cell Seeding Number per (micro-)well/drop	Timepoint of Imaging (h)	Number of Images
Axiovert 200	BT20	DMEM LG	Liquid Overlay: Agarose coated	0,5/1/1,5/2/4/5/6/10	96	70
	BT474		Liquid Overlay: Agarose coated	3	96	14
	DLD1		Liquid Overlay: Agarose coated	3/3,5/4/4,5/5	96	85
	HCT15		Liquid Overlay: Agarose coated	3,5/4/4,5/5/5,5/6	96	134
	Hs578T		Liquid Overlay: Agarose coated	0,5/1/4/9/10/11/12/13	96	80
	MDAMB361		Liquid Overlay: Agarose coated	5/6/7	96	33
	NCIH226		Liquid Overlay: Agarose coated	0,5/1/1,5/2/3/4	96	148
	OVCAR8		Liquid Overlay: Agarose coated	0,5/1/1,5/2/3/4	96	140
Axiovert 200M	4T1	DMEM HG / RPMI1640 / RPMI1640 / DMEM LG	Liquid Overlay: ULA-plate	2	168	116
	A549		Liquid Overlay: ULA-plate	2/4/6/8	168	470
	BEAS2B		Liquid Overlay: ULA-plate	2	168	18
	BT474		Liquid Overlay: Agarose coated	3	96	9
	CAL33		Liquid Overlay: Agarose coated	1/2/3/4/5/6/7/8/9	96	64
	FaDu		Liquid Overlay: Agarose coated	1,2/1,8/2,5/4,5/ 6/8/10/12	96	64
	HCA2hTert		Liquid Overlay: ULA-plate	2	168	25
	HCC2998		Liquid Overlay: Agarose coated	1,75	168	16
	HCT116		Liquid Overlay: ULA-plate	0,5/1/2/3	168	597
	HEK293		Liquid Overlay: Agarose coated	3/4/5/6/7	96	42
	HEPG2		Liquid Overlay: ULA-plate	2	168	68
	HOP62		Liquid Overlay: Agarose coated	2/3/4/5/6	96	48
	HSC4		Liquid Overlay: Agarose coated	1/2/3/4/5/6/7/8	96	44
	MCF7		Liquid Overlay: ULA-plate	2	168	99
	MDAMB361		Liquid Overlay: Agarose coated	8	96	8
	NCIH226		Liquid Overlay: Agarose coated	1,75	96	20
	NCIH460		Liquid Overlay: Agarose coated	0,4/0,5/0,6/0,8/ 1/1,5/2/4	96	67
	OVCAR8		Liquid Overlay: Agarose coated	2	96	16
	PANC1		Liquid Overlay: ULA-plate	2	168	135
	PATU8902		Liquid Overlay: Agarose coated	0,5/1,5/3/4/6	96	37
	SAR030		Liquid Overlay: ULA-plate	8	168	119
	SAR121		Liquid Overlay: ULA-plate	2	168	53
	SAS		Liquid Overlay: Agarose coated	0,6/0,8/1,5/2/ 2,5/3/4/5	96	67
	SKOV3		Liquid Overlay: ULA-plate	2/4/6/8	168	401
	SW1353		Liquid Overlay: ULA-plate	2	168	86
	U87MG		Liquid Overlay: ULA-plate	2/4/6/8	168	371
	U138MG		Liquid Overlay: Agarose coated	1,5/8/9/10	96	31
	U251MG		Liquid Overlay: Agarose coated	9/10/11	96	16
Cytation 5	CT5.3hTERT		Liquid Overlay: ULA-plate	6	48	66
Incucyte S3	MCF10A	DMEM/F-12 Matrigel / DMEM/F-12 BME	Liquid Overlay: Agarose coated	3	0-374	468
Incucyte Zoom	4T1		Hanging Drop / Liquid Overlay: ULA-plate	2	72	16
	A549			2	72	184
	D2A1LUCmCherry			2	72	30
	HCT116			2	72	170
	HEPG2			2	72	87
	PANC1			2	72	108
	SKOV3			2	72	147
Leica DMi 1	SW837		Liquid Overlay: Microchip	1/2/5/8/10/15/20	24-360	2317
Leica DMi3000 B	4T1LUC		Liquid Overlay: Microchip	0,158/0,315/0,631/ 0,946/1,262	24-168	21
	ASC			0,315/0,631/ 0,946	24-144	59
	MDAMB231			0,315/0,631/ 0,946	24-168	21
	A549		Hanging Drop	2	72	55
	D2A1LUCmCherry					32
	HCT116					88
	HEPG2					62
	PANC1					33
	SKOV3					44
	T47D					24
Olympus IX05	A549-MRC5		Liquid Overlay: ULA-plate	4	168	22
	H1299			2	168	19
	MRC5			10	72	23
	VCaP			2	168	24
Opera Phenix	HeLa		Liquid Overlay: Agarose coated	2	96	14
	HuH7					15
	LNCap					15
	MDCK					15

Table 1. Summary of SLiMIA content. BME, basement membrane extract.

Cell Line	Supplier	2D Culture Condition									STR profile confirmation (Yes/No)
		Medium	Glucose concentration (g/l)	Antibiotics (% P/S)	HEPES (mM)	Other Supplements	Serum Type	Serum concentration (%)	Heat-inactivated (Yes/No)	CO_2 (%)	
4T1	ATCC	DMEM HG	4.5	1	—	—	FBS	10	Yes	5	N/A
4T1LUC	ATCC	DMEM HG	4.5	1	—	—	FBS	10	Yes	5	N/A
A549	ATCC	DMEM HG	4.5	1	—	—	FBS	10	Yes	5	Yes
ASC	Sigma	DMEM HG, Glutamax	4.5	0.5	—	—	FBS	10	Yes	5	Yes
BEAS2B	ATCC	DMEM HG	4.5	1	—	—	FBS	10	Yes	5	Yes
BT20	ATCC	DMEM LG	1	1	—	—	FBS	10	Yes	5	Yes
BT474	Tumorbank Heidelberg	DMEM LG	1	1	—	—	FBS	10	Yes	5	Yes
CAL33	Leibniz Institute DSMZ	DMEM LG	1	1	25	—	FBS	10	Yes	5	Yes
CT5.3 hTERT	Primary, immortalized (hTERT transfection)	DMEM HG	4.5	1	—	—	FBS	10	Yes	10	Yes
D2A1LUCmCherry	Gift from Clare Isacke, London, UK	DMEM HG	4.5	1	—	—	FBS	10	Yes	5	N/A
DLD1	ATCC	DMEM LG	1	1	—	—	FBS	10	Yes	5	Yes
FaDu	ATCC (Dresden subline)	DMEM LG	1	1	25	—	FBS	10	Yes	8	Yes
H1299	ATCC	RPMI	2	/	—	1% Glutamine, 0,1% insulin	FBS	10	No	5	Yes
HCA2hTERT	Gift from C. Jones, Cardiff, UK	DMEM HG	4.5	1	—	—	FBS	10	Yes	5	Yes
HCC2998	NCI	DMEM LG	1	1	—	—	FBS	10	Yes	5	Yes
HCT15	ATCC	DMEM LG	1	1	—	—	FBS	10	Yes	5	Yes
HCT116	ATCC	DMEM HG	4.5	1	—	—	FBS	10	Yes	5	Yes
HEK293	ATCC	DMEM LG	1	1	—	—	FBS	10	Yes	5	Yes
HeLa	Tebu-bio	RPMI	2	1	—	—	FBS	10	No	5	Yes
HEPG2	ATCC	DMEM HG	4.5	1	—	—	FBS	10	Yes	5	Yes
HOP62	NCI	DMEM LG	1	1	—	—	FBS	10	Yes	5	Yes
Hs578T	ATCC	DMEM LG	1	1	—	—	FBS	10	Yes	5	Yes
HSC4	JCRB/HSRRB (Japan)	DMEM LG	1	1	25	—	FBS	10	Yes	5	Yes
HuH7	CLS (Cell line service GmbH, Eppelheim, Germany)	RPMI	2	1	—	—	FBS	10	No	5	Yes
LNCap	CLS	RPMI	2	1	—	—	FBS	10	No	5	Yes

Continued

Cell Line	Supplier	2D Culture Condition									STR profile confirmation (Yes/No)
		Medium	Glucose concentration (g/l)	Antibiotics (% P/S)	HEPES (mM)	Other Supplements	Serum Type	Serum concentration (%)	Heat-inactivated (Yes/No)	CO_2 (%)	
MCF7	ATCC	DMEM HG	4.5	1	—	—	FBS	10	Yes	5	Yes
MCF10A	ATCC	DMEM/F12	3.15	1	—	0,5 µg/ml hydrocortisone; 20 ng/ml HB-EGF; 100 ng/ml Cholera Toxin; 10 µg/ml insulin	Horse Serum	5	No	5	Yes
MDAMB231	ATCC	DMEM HG	4.5	1	—	—	FBS	10	Yes	5	Yes
MDAMB361	ATCC	DMEM LG	1	1	—	—	FBS	10	Yes	5	Yes
MDCK	CLS	RPMI	2	1	—	—	FBS	10	No	5	N/A
MRC5	ATCC	EMEM	1	/	—	—	FBS	10	No	5	Yes
NCIH226	ATCC	DMEM LG	1	1	—	—	FBS	10	Yes	5	Yes
NCIH460	ATCC	DMEM LG	1	1	—	—	FBS	10	Yes	5	Yes
OVCAR8	NCI	DMEM LG	1	1	—	—	FBS	10	Yes	5	Yes
PANC1	ATCC	DMEM HG	4.5	1	—	—	FBS	10	Yes	5	Yes
PaTu8902	DSMZ	DMEM LG	1	1	25	—	FBS	10	Yes	8	Yes
SAR030	Primary, early-passage	DMEM HG	4.5	1	—	—	FBS	10	Yes	5	Yes
SAR121	Primary, early-passage	DMEM HG	4.5	1	—	—	FBS	10	Yes	5	Yes
SAS	JCRB/HSRRB (Japan)	DMEM LG	1	1	25	—	FBS	10	Yes	8	Yes
SKOV3	ATCC	DMEM HG	4.5	1	—	—	FBS	10	Yes	5	Yes
SW837	ATCC	DMEM/F12	3.15	1	—	—	FBS	10	Yes	5	Yes
SW1353	ATCC	DMEM HG	4.5	1	—	—	FBS	10	Yes	5	Yes
T47D	ATCC	DMEM HG	4.5	1	—	—	FBS	10	Yes	5	Yes
U87MG	ATCC	DMEM HG	4.5	1	—	—	FBS	10	Yes	5	Yes
U138MG	CLS	MEM	1	1	25	—	FBS	10	Yes	5	Yes
U251MG	CLS	MEM	1	1	25	—	FBS	10	Yes	5	Yes
VCaP	ATCC	DMEM HG	4.5	/	—	—	FBS	10	No	5	Yes

Table 2. 2D cell culture conditions. Summary of culture conditions prior to spheroid formation. N/A, not applicable.

Microscope				Objective(s)					Camera			Software	
Model	Brand	Lab	Microscopic technique	Brand	Magnification	Immersion Medium	Nominal Aperture (NA)	Working Distance (WD, in mm)	Type	Resolution (pixels)	Scale (pixel/µm)	Name	Version
Axiovert 200	Zeiss	Kunz-Schughart	Phase-contrast	Zeiss	10x	Air	0.3	5.2	AxioCamMRc	1300 × 1030	1.5408	KS300	3.0
Axiovert 200 M	Zeiss	De Wever	Phase-contrast	Zeiss	10x	Air	0.25	4.2	AxioCam HRm	1300 × 1030	0.9398	Axiovision	SE64Rel.4.7
		Kunz-Schughart	Phase-contrast	Zeiss	5x	Air	0.12	18.5	AxioCamMR	1300 × 1030	0.4900	Axiovision	SE64Rel.4.5
		Kunz-Schughart	Phase-contrast	Zeiss	10x	Air	0.3	5.2	AxioCamMR	1300 × 1030	0.9699	Axiovision	SE64Rel.4.5
Cytation 5	Agilent	De Wever	Brightfield	Olympus	4x	Air	0.13	17	Sony IMX 264 CMOS	1992 × 1992	0.5734	Gen5	3.14
IncucyteS3	Sartorius	Takayama	Phase-contrast	Nikon	10x	Air	0.3	7.2	CMOS	1408 × 1040	0.8000	IncuCyte	V2019B Rev2
IncucyteZoom	Sartorius	De Wever	Phase-contrast	Nikon	10x	Air	0.3	16.0	Basler Sca	1392 × 1038	0.8197	IncuCyte	V2019B
Leica DMI1	Leica	Cruz	Brightfield	Leica	10x	Air	0.22	45.0	Leica MC170 HD	2592 × 1944	2.0000	LAS software	/
Leica DMI3000 B	Leica	De Wever	Phase-contrast	Leica	5x	Air	0.12	14.0	Leica DFC350 FX	1600 × 1200	0.6250	LAS software	/
Olympus IX05	Olympus	Tesei	Brightfield	Olympus	4x	Air	0.13	17.0	Nikon Digital Sight DS-Vi1	800 × 600	0.2988	NIS Elements D	ver. 4.10
Opera Phenix	Perkin Elmer	Steigemann	Brightfield	Zeiss	10x	Air	0.3	5.2	sCMOS	1080 × 1080	0.8354	Harmony	4.9

Table 3. Microscopy set-up. Set-up for each microscope, including objectives, camera system and software details.

All human cell lines were authenticated via STR profiling (ATCC, United States; DSMZ, Germany; Eurofins, Luxembourg; Genomic Scientific Platforms, i3S, Portugal; Institute of Legal Medicine, TU Dresden, Germany) and routinely tested to exclude Mycoplasma contamination.

Spheroid formation.

a. Liquid overlay: Ultra-Low Attachment (ULA) plate

4T1, A549, BEAS2B, CT5.3 hTERT, D2A1LUCmCherry, HCA2hTERT, HCT116, HEPG2, MCF7, PANC1, SAR030, SAR121, SKOV3, SW1353 and U87MG

The U-shaped, 96-well (CLS7007-24EA, Sigma-Aldrich, Saint Louis MO, USA) and 384-well (MS-9384UZ, S-bio, Hudson NH, USA) ultra-low attachment (ULA) plates were seeded in a suspension of respectively 200 µl or 80 µl cell culture media with different seeding densities (Table 1). Culture media were DMEM high glucose (HG) (41965039, ThermoFisher), DMEM/F12 (1:1) (41965039 and 21765029, ThermoFisher), RPMI1640 (21875091, ThermoFisher), DMEM low glucose (LG) (31885023, ThermoFisher), EMEM (10-009-CV, Corning) and MEM (10370-047, ThermoFisher), all supplemented with 10% FBS, 100IU/ml penicillin and 100 mg/ml streptomycin (P/S). The ULA plates were sealed with Breathe-Easy semipermeable tape (BEM-1, Dedham MA, USA) to prevent evaporation. The spheroids were cultured at 37 °C in an atmosphere of 5% CO_2 under normoxia.

MCF10A: BME, Matrigel

To culture MCF10A mammary 3D spheroids, MCF10A cells were seeded in 384-well U-shaped ULA (#MS-9384UZ, S-bio, Hudson, NH, USA) plate. We have previously reported the use of 384-well culture platforms to form MCF10A spheroids and refer to the culture protocol[21–23]. Briefly, MCF10A cells were cultured in growth media containing DMEM/F12 (11330-032, Gibco) and supplemented with 5% horse serum (16050-122, Gibco), 20 ng/ml HB-EGF (100-47, Peprotech), 0.5 µg/ml hydrocortisone (H0888, Sigma), 100 ng/ml Cholera toxin (C8052, Sigma), and 10 µg/ml insulin (I1882, Sigma). 2D cultures were maintained at 37 °C and 5% CO2 in T75 culture flasks, supplemented with 1% P/S (15140-163, Gibco), and routinely passaged at 70–80% confluence. To culture 3D spheroid formation in 384-well ULA plate 3×10^3 MCF10A cells were seeded in each well in a final volume of 25 µl[22]. The cells were supplemented with 0.24% methocel A4M (94378, Sigma), 10% FBS (900-108, GemiBio), 120 µg/ml Matrigel™ (256231, Corning) or 100 µg/ml Cultrex UltiMatrix Basement Membrane Extract (BME001-01, R&D system). On day 3 of spheroid culture, the media was exchanged 3 times to wash out the seeding supplements using a CyBio FeliX liquid handling machine (Analytik Jena). For routine culture, media was exchanged 2 times every 2-3 days. While the spheroids were maintained in ULA culture, they were imaged using an Incucyte S3 (Sartorious) in-incubator microscope system.

A549-MRC5, H1299, MRC5, VcaP

U-bottom 96-well (CLS7007-24EA, Sigma-Aldrich, Saint Louis MO, USA) and 384-well (MS-9384UZ, S-bio, Hudson NH, USA) ULA plates were seeded with a suspension of 80 µl cell culture media with 2×10^3 (H1299, VCAP cells) and 10×10^3 (MRC5 cells). About the heterotypic multicellular spheroids composed by A549 and MRC5 cells, a mixed suspension of 80 µl cell culture media with both cell lines in a 1:1 ratio was used (*i.e.* 2×10^3 A549:2×10^3 MRC5). Culture media were: RPMI (ECB9006, Euroclone) supplemented with 1% L-glutamine, 0.1% Insulin for H1299 cells; EMEM (30–2003, ATCC) for MRC5 and A549-MRC5 spheroids and DMEM high glucose (41965039, ThermoFisher) for VCAP. All culture media were supplemented with 10% FBS and without antibiotic/antimycotic. The ULA plates were sealed with Breathe-Easy semipermeable tape (BEM-1, Dedham MA, USA) to prevent evaporation. The spheroids were cultured at 37 °C in an atmosphere of 5% CO_2 under normoxia.

b. Liquid overlay: agarose-coated plate

BT20, BT474, CAL33, DLD1, FaDu, HCC2998, HCT15, HEK293, HOP62, Hs578T, HSC4, MDAMB361, NCIH226, NCIH460, OVCAR8, PaTu8902, SAS, U138MG, U251MG

Spheroids from these cells lines derive from spheroid experiments using the liquid-overlay approach in flat-bottom 96-well plates coated with 50 µl/well of 1.5% agarose in serum-free medium (A8539-100G, Sigma Aldrich) as described in Friedrich *et al.*[24], with all materials and distributors as detailed. In brief, all epithelial cancer cell types were routinely grown in DMEM with physiological (low) glucose concentration (LG), with or without 25 mM HEPES (P04-05551 and P04-01550 respectively, Pan Biotech), supplemented with 10% heat-inactivated FBS, 100 IU/ml penicillin and 100 mg/ml streptomycin (1% P/S) (Pan Biotech). U138-MG and U251 glioblastoma cell lines and spheroids were cultured in MEM Eagle with EBSS (P04-08250, Pan Biotech), supplemented with 10% FBS and antibiotics (1% P/S). Spheroids were formed by seeding single cell suspensions on the agarose-coated wells and were kept at 37 °C, normoxia, 5% or 8% CO2, as highlighted in Tables 1, 2.

Hela, HuH7, LNCap, MDCK

Spheroid formation was carried out using a modified version of the liquid overlay technique[25]. 10 µl of a heated 1.5% w/v agarose (in DMEM (11880036, ThermoFischer), without FBS) solution was dispended by liquid dispensers (Multidrop Combi, Thermo Scientific) into sterile 384-well clear bottom imaging plates (6057308,

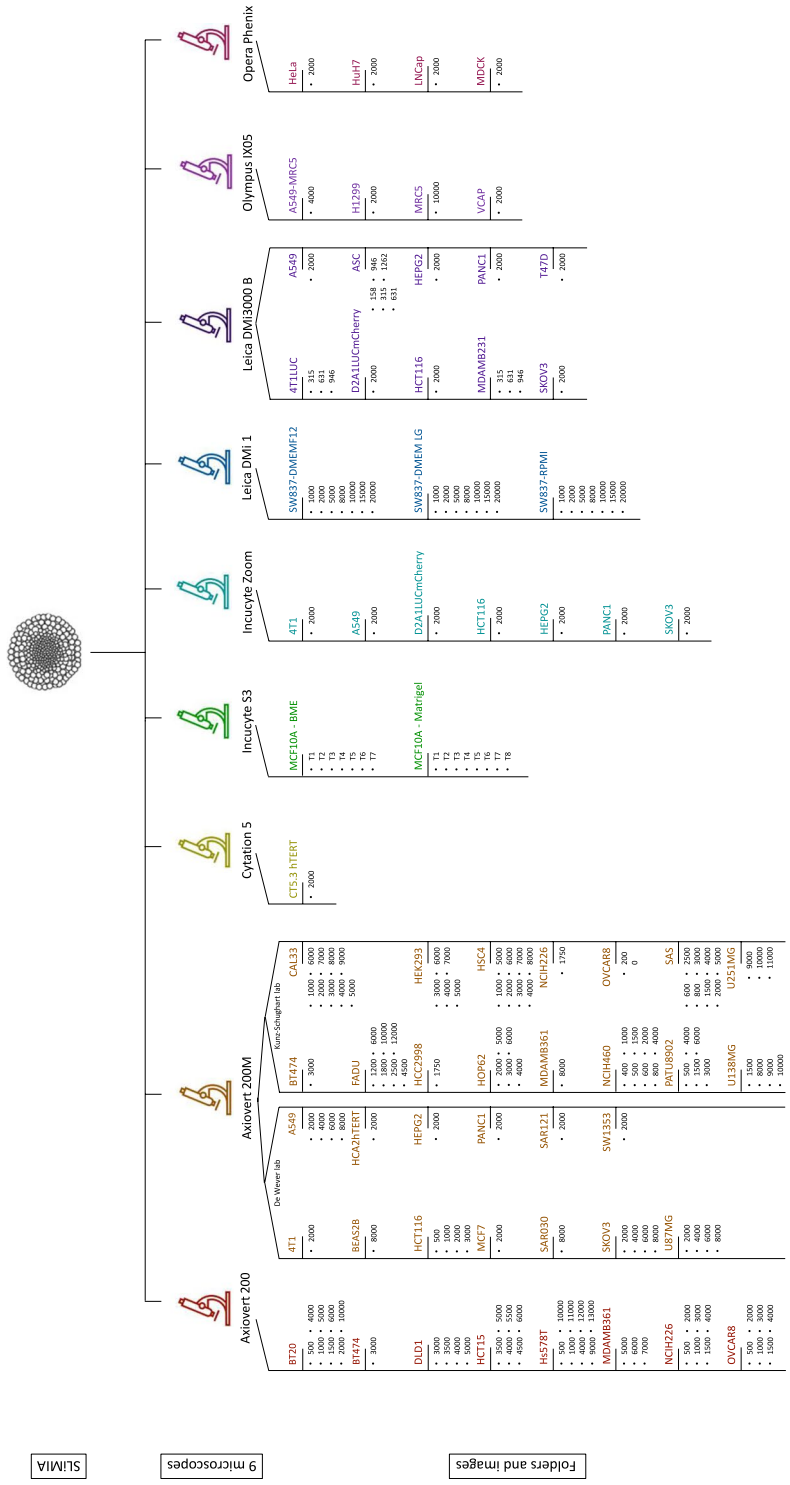

Fig. 3 Structure of SLiMIA. SLiMIA is subdivided into 9 microscopes where each microscope folder contains a folder with images and a mirroring folder with the corresponding manual segmentations. In the second level each microscope folder is subdivided in cell line folders. One level lower, folders are named by the cell seeding density per well/drop. Except for Incucyte S3 where T1-T7 represent technical replicates of spheroids followed over time (0–374 h).

Perkin Elmer) and cooled down at room temperature. Next, single cell suspensions were seeded in 40 µl RPMI1640 (21875-034, Gibco) containing 10% FBS supplemented with 1% P/S using a liquid dispenser. The plates were then incubated under standard cell culture conditions at 37 °C and 5% CO2 in humidified incubators.

c. Liquid overlay: Microchip

4T1LUC, ASC, MDAMB231

Agarose microchips with 400 µm diameter pores were prepared as follows: 3 g UltraPure Agarose (16500-500, Invitrogen) was dissolved in 100 ml sterile PBS^- by heating, resulting in a 3% w/v agarose solution. This solution was poured over a negative polydimethylsiloxane (PDMS) mold (height 3 mm, diameter 18 mm) which contains 1585 (400 µm) pores. Once solidified, the agarose microchips were separated from their molds and placed in a 12-well plate. Next, 500 µl of cell suspension was seeded onto the 400 µm pore microchip.

SW837

Agarose microchips with 800 µm diameter pores were prepared as follows: 2 g SeaKem® LE Agarose (50004, Lonza) was dissolved in 100 ml sterile 0.9% NaCl by heating, resulting in a 2% w/v agarose solution. This solution was poured over a MicroTissues® 3D Petri Dish micro-mold (Z764000-6EA, Merck) which contains 81 pores. Once solidified, the agarose microchips were separated from their molds and placed in a 12-well plate. Next, 190 µl of cell suspension SW837 was seeded onto the microchip.

d. Hanging drop

In the hanging drop method, 2×10^3 cells were plated under the lids of petri dishes (A19618, Novolab, Geraardsbergen, Belgium) in 20 µl drops of DMEM HG (41965039, ThermoFisher) or DMEM LG (31885023, ThermoFisher). The bottom of the petri dishes was filled with 10 ml $PBSD^-$ to limit evaporation.

Light microscope. Each applied microscopic set-up (microscope, objectives, camera system and acquisition software) is summarized in Table 3.

Image processing and statistics. AnaSP (v1.4) has been applied to segment the spheroid images and extract morphological parameters[26]. Principal component analysis (PCA) was performed in Graphpad Prism (v9.3.1) with 11 cell lines which are representative for the various morphological types of spheroids and of which sufficient biological ($\geq$3) and technical ($\geq$6) were obtained. These spheroids were all cultured in ULA plates (cfr. supra).

Manual segmentation. Each light microscopy image underwent manual segmentation. In AnaSP (v1.4)[26] the authors and contributors manually segmented the spheroid images, distinguishing foreground (spheroid) from background. For the manual segmentation the spheroid images are enlarged to optimally distinguish foreground from background. This segmentation results in a binary (B/W) ome.tiff image with the identical name as the original raw image. These manual segmentation images can be thus considered as ground truth images.

Image conversion. To retain a maximum amount of metadata, to facilitate handling of multidimensional pixel information (e.g. for annotation and deep learning workflows) and to create uniformity the microscopic images were converted from a .jpg- or .tiff- to an ome.tiff-format by use of bftools (Bio-Formats, v5.6.0).

Data Records

SLiMIA is accessible at Figshare[5]. Figure 3 demonstrates that SLiMIA consists of 3 levels. In the first level, the atlas is subdivided in 9 folders named by microscope (e.g. Axiovert 200, Incucyte S3) where each microscope folder contains a folder with images and a mirroring folder with the corresponding manual segmentations. In the second level, folders are named by the cell line of the spheroids (e.g. BT20, BT474, DLD1). In the third level, folders are described by the cell seeding density applied to form spheroids (e.g. 800, 1000, 2000). Except for Incucyte S3 where T1-T7 represent technical replicates of spheroids followed over time. The last level holds the spheroid images. To provide as much metadata as possible per image, each image file is named as follows:

"CELLLINENAME_CULTUREMEDIUM_FormationMethod_CellSeedingDensity_TimepointOfImaging_BiologicalReplicateNumber_TechnicalReplicateNumber_Magnification.ome.tiff"

For example:

D2A1LUCmCherry_DMEMLG_HangingDrop_2000cells_72h_B1_T5_10x.ome.tiff

The images contain raw data only. No processing has occurred apart from image conversion to grayscale and to ome.tiff.

Technical Validation

Two independent observers (AP, SK) visually verified the quality of the images with special attention for focus, inclusion of all spheroid borders, absence of non-cellular (e.g. dust) particles which could interfere with spheroid structure. Images that did not qualify were removed from the dataset. Brightness and contrast were evaluated on a second level since these parameters are easily adjustable through most image software packages.

Code availability

No custom code was utilized in this work. Some versions of ImageJ need the Bio-Formats plugin to open ome.tiff files (https://www.openmicroscopy.org/bio-formats/downloads/).

Received: 22 January 2023; Accepted: 9 January 2025;
Published online: 17 February 2025

References

1. Hirschhaeuser, F. *et al*. Multicellular tumor spheroids: an underestimated tool is catching up again. *J. Biotechnol.* **148**, 3–15 (2010).
2. Han, K. *et al*. CRISPR screens in cancer spheroids identify 3D growth-specific vulnerabilities. *Nature* **580**, 136–141 (2020).
3. Folkesson, E. *et al*. High-throughput screening reveals higher synergistic effect of MEK inhibitor combinations in colon cancer spheroids. *Sci. Rep.* **10**, 11574 (2020).
4. Peirsman, A. *et al*. MISpheroID: a knowledgebase and transparency tool for minimum information in spheroid identity. *Nat. Methods* **18**, 1294–1303 (2021).
5. Blondeel, E. *et al*. SLiMIA: the Spheroid Light Microscopy Image Atlas. *Figshare* https://doi.org/10.6084/m9.figshare.c.7486311 (2024).
6. You, L. *et al*. Linking the genotypes and phenotypes of cancer cells in heterogenous populations via real-time optical tagging and image analysis. *Nat. Biomed. Eng.* **6**, 667–675 (2022).
7. Mousavikhamene, Z., Sykora, D. J., Mrksich, M. & Bagheri, N. Morphological features of single cells enable accurate automated classification of cancer from non-cancer cell lines. *Sci. Rep.* **11**, 24375 (2021).
8. Falk, T. *et al*. U-net: deep learning for cell counting, detection, and morphometry. *Nat. Methods* **15**, 67–70 (2019).
9. Hammer, M. *et al*. Towards community-driven metadata standards for light microscopy: tiered specifications extending the OME model. *Nat. Methods* **18**, 1427–1440 (2021).
10. Boehm, U. *et al*. QUAREP-LiMi: a community endeavor to advance quality assessment and reproducibility in light microscopy. *Nat. Methods* **18**, 1423–1426 (2021).
11. Wilkinson, M. D. *et al*. The FAIR guiding principles for scientific data management and stewardship. *Sci. Data* **3**, 160018 (2016).
12. Streller, M. *et al*. Image segmentation of treated and untreated tumor spheroids by fully convolutional networks. *Preprint at* https://arxiv.org/pdf/2405.01105 (2024).
13. Li, S. *et al*. Simultaneous 2D and 3D cell culture array for multicellular geometry, drug discovery and tumor microenvironment reconstruction. *Biofabrication* **13** (2021).
14. Bairoch, A. The cellosaurus, a cell-line knowledge resource. *J. Biomol. Tech.* **29**, 25–38 (2018).
15. De Boeck, A. *et al*. Differential secretome analysis of cancer-associated fibroblasts and bone marrow-derived precursors to identify microenvironmental regulators of colon cancer progression. *Proteomics* **13**, 379–388 (2013).
16. De Wever, O. *et al*. Tenascin-C and SF/HGF produced by myofibroblasts *in vitro* provide convergent proinvasive signals to human colon cancer cells through RhoA and Rac. *FASEB J.* **9**, 1016–1018 (2004).
17. De Vlieghere, E. *et al*. Tumor-environment biomimetics delay peritoneal metastasis formation by deceiving and redirecting disseminated cancer cells. *Biomaterials* **54**, 148–157 (2015).
18. Jungwirth, U. *et al*. Generation and characterisation of two D2A1 mammary cancer sublines to model spontaneous and experimental metastasis in a syngeneic BALB/c host. *Dis. Model Mech.* **11** (2018).
19. Wyllie, F. *et al*. Telomerase prevents the accelerated cell ageing of Werner syndrome fibroblasts. *Nat. Genet.* **24**, 16–17 (2000).
20. Fischer, S. *et al*. Post-operative minimal residual disease models to study metastatic relapse in soft-tissue sarcoma patient-derived xenografts. *Clin. Transl. Med.* **13**, e1290 (2023).
21. Parigoris, E. *et al*. Cancer cell invasion of mammary organoids with basal-in phenotype. *Adv. Healthc. Mater.* **10**, 2000810 (2021).
22. Lee, S. *et al*. High-throughput formation and image-based analysis of basal-in mammary organoids in 384-well plates. *Sci. Rep.* **12**, 317 (2022).
23. Djomehri, S. I., Burman, B., Gonzalez, M. E., Takayama, S. & Kleer, C. G. A reproducible scaffold-free 3D organoid model to study neoplastic progression in breast cancer. *J. Cell Commun. Signal.* **13**, 129–143 (2019).
24. Friedrich, J., Seidel, C., Ebner, R. & Kunz-Schughart, L. A. Spheroid-based drug screen: considerations and practical approach. *Nat. Protoc.* **4**, 309–324 (2009).
25. Wenzel, C. *et al*. 3D high-content screening for the identification of compounds that target cells in dormant tumor spheroid regions. *Exp. Cell Res.* **323**, 131–143 (2014).
26. Piccinini, F. AnaSP: A software suite for automatic image analysis of multicellular spheroids. *Comput. Methods Programs Biomed.* **119**, 43–52 (2015).

Acknowledgements

Thanks to Marit Wondrak for the technical assistance in spheroid culturing. Anouk Vanderstricht, Taylor N. Brinsfield, Mariachiara Stellato, Noah Borges, Carolien Sels, Oscar Lemmens and Sabina Shamieva helped in the manual annotation of the atlas. ODW acknowledges support by the Concerted Research Actions from Ghent University, Stichting Tegen Kanker (Foundation against Cancer), Kom Op Tegen Kanker (Stand up to Cancer), the Flemish cancer society, and Fund for Scientific Research Flanders. FP and GC acknowledge support from the MAECI Science and Technology Cooperation Italy-South Korea Grant Years 2023–2025 by the Italian Ministry of Foreign Affairs and International Cooperation (CUP project: J53C23000300003).

Author contributions

A.P. and O.D.W. designed the study. O.D.W., A.T., S.T., P.S., L.K.S. and M.J.O. supervised experiments. E.B., A.P., F.D.V., S.A.J., M.B., T.C., D.E., S.L., N.M. and N.Z. collected data. F.P. and G.C. designed software. S.K., S.T., S.L., N.M., M.B., E.B., F.P., G.C., F.D.V., A.P., D.E., T.C., M.J.O. and S.V. manually annotated images. A.P., S.V. and S.D. processed the data. A.P., E.B., S.V., F.P., P.B., G.C., T.C., L.D.M., M.J.O., L.K.S., P.S., S.T., A.T. and O.D.W. edited the manuscript. E.B., A.P. and S.V. contributed equally.

Competing interests

The authors declare no competing interests.

Additional information

Correspondence and requests for materials should be addressed to A.P. or O.D.W.